Rapid Mapping of Morphological Change Following the 2024 Ruang Volcano Eruption Using Multi-sensor Remote Sensing Imagery

Donna Monica
National Research and Innovation Agency

Imam Santoso
National Research and Innovation Agency

Suwarsono Suwarsono
National Research and Innovation Agency

Yenni Vetrita
National Research and Innovation Agency

他

https://doi.org/10.5109/7388839

出版情報：Evergreen. 12 (3), pp.1426-1437, 2025-09. 九州大学グリーンテクノロジー研究教育センター
バージョン：

Rapid Mapping of Morphological Change Following the 2024 Ruang Volcano Eruption Using Multi-sensor Remote Sensing Imagery

Donna Monica[1,*], Imam Santoso[1], Suwarsono[1], Yenni Vetrita[1], Arum Tjahyaningsih[1], Farikhotul Chusnayah[1], Rido Dwi Ismanto[1], Rahmadi[1], Mamat Suhermat[1], Heruningtyas Desi Purnamasari[2], Herlan Darmawan[3]

[1]National Research and Innovation Agency, Gedung B.J. Habibie, Jl. M.H. Thamrin No. 8, Jakarta Pusat 10340, Indonesia
[2]Center of Volcanology and Geological Hazard Mitigation, Jl. Diponegoro No.57, Cihaur Geulis, Cibeunying Kaler, Bandung, Jawa Barat 40122, Indonesia
[3]Laboratory of Geophysics, Universitas Gadjah Mada, Jalan Sekip Utara, Sendowo, Sinduadi, Kec. Mlati, Kabupaten Sleman, Daerah Istimewa Yogyakarta 55281, Indonesia

*Author to whom correspondence should be addressed:
E-mail: donna.monica@brin.go.id

(Received October 02, 2024; Revised July 02, 2025; Accepted August 15, 2025)

Abstract: Ruang Volcano in North Sulawesi, Indonesia, experienced two significant eruptions in April 2024, producing widespread pyroclastic flows and sulfur dioxide emissions that affected areas over 90 km away. Ruang volcano has a history of deathly eruption in 1871 when a tsunami was triggered and caused the deaths of over 400 people. Such history underlines the need to monitor the recent Ruang volcanic activities and associated risks closely. This study demonstrates the integration of high-resolution PlanetScope optical imagery and Sentinel-1A SAR data for near real-time assessment of morphological changes during the 2024 eruption. We show that this multi-sensor approach provides complementary insights: Visual inspection on PlanetScope data captures fine-scale surface features, while interferometric and backscatter analysis on the cloud-penetrating Sentinel-1A data reveals deformation information. Our analysis reveals substantial shoreline expansion (20–70 meters) and elevation changes −0.341 to 0.138 meters) along Ruang's east and west coasts. These coastal morphological shifts may enhance the risk of tsunami generation, particularly under future scenarios involving flank collapse or continued deformation. The results show the potential of integrated remote sensing frameworks for rapid hazard assessment and early warning in volcanically active regions.

Keywords: PlanetScope; Quick response monitoring; remote sensing; Ruang volcano; Sentinel-1A

1. Introduction

On 16 April 2024, the Ruang volcano in North Sulawesi, Indonesia, erupted just hours after its alert status was raised. The explosion released lava, ash, sulfur dioxide, and other materials. Although the alert level was downgraded days later, another major eruption occurred on 30 April, causing volcanic rock showers that led to the closure of Sam Ratulangi Airport which is located approximately 97.3 kilometers away, and SO2 emissions reaching as far as Kalimantan Island. Historically, Ruang volcano had its most catastrophic eruption in 1871, causing a tsunami that resulted in the deaths of over 400 people[1)]. The second to most recent eruption was 22 years ago in 2002 which caused damage to settlements and agricultural land, resulting in 1000 people evacuated to nearby islands[2)]. Considering this history, it is necessary to closely monitor Ruang volcano's activities. The 2024 eruption of Ruang volcano requires careful observation and detailed analysis, especially regarding its morphological changes and potential tsunami risks.

During volcanic disasters, regions affected by eruptions are often rendered inaccessible due to the presence of hazardous conditions such as pyroclastic flows, ashfall,

Cite: D. Monica et al., "Rapid Mapping of Morphological Change Following the 2024 Ruang Volcano Eruption Using Multi-sensor Remote Sensing Imagery". Evergreen, 12 (03) 1426-1437 (2025). https://doi.org/10.5109/7388839.

and unstable terrain[3,4]. These challenges are especially true for Ruang volcano, located on a small remote island in northern Indonesia. The ground monitoring becomes limited and even impossible. This logistical difficulty associated with accessing such locations make it necessary to employ remote sensing technologies for effective monitoring and risk assessment. Remote sensing enables acquisition of consistent, near real time observation data. Thus, continuous real-time monitoring of volcanic activity relies heavily on remote sensing[5]. Remote sensing provides essential data for monitoring, assessment, and rapid mapping when physical access is limited[6]. The use of multisensor data enhances the ability to analyze volcanic morphology during critical times[7].

Multisensor remote sensing has been employed to provide comprehensive data for mapping and monitoring volcanic activities[8,9]. Thermal sensors such as MODIS is used to monitor a volcano's thermal activities over the years and detect anomalies that may be signs for an eruption[10,11]. In more recent research, VIIRS data is slowly replacing MODIS in thermal monitoring[12]. Campus et al. compare both data and conclude that VIIRS data has a better quality of radiance value compared to MODIS which results in better anomaly detection[13]. Likewise, other thermal data with higher spatial resolution but lower temporal resolution such as Sentinel-2 SWIR (Shortwave Infrared) data[14,15] and Landsat-8 TIRS[16] are used to detect volcanic hotspots as well. Aside from thermal sensor data, SAR (Synthetic Aperture Radar) data is also widely used in volcanic mapping and monitoring. Biggs et al. analyzed five years data of Turkish volcanoes using Sentinel-1 to find early-stage signs of volcanic activities[17]. In the post-eruption analysis, Tiengo et al. employed Sentinel-1 GRD data to identify and map the lava flow of the 2014 Fogo volcano eruption[18].

To date, there is a lack of specific case studies on remote sensing usage on Ruang volcano monitoring, probably due to its prolonged dormancy. However, the recent eruption raised the urgency for such research. Furthermore, Ruang location in the tropical region poses a cloud cover issue which complicates continuous monitoring with optical remote sensing data[19]. PlanetScope, for example, may offer daily high-resolution imagery, but its usefulness is diminished as a result. Conversely, radar satellites like Sentinel-1 can penetrate cloud cover and deliver data every 12 days, but the lower temporal resolution limits the ability to capture rapid changes. Therefore, an integration of multi-sensor data is needed to overcome the limitations of those data.

This study evaluates the use of multi-sensor remote sensing data for detecting and mapping volcanic morphological changes, with a focus on identifying the best approach on the use of multi-sensor datasets to deliver near real-time insights on the 2024 Ruang eruption.

2. Proposed method

2.1. Study Area

Ruang volcano is an active volcano located on Ruang Island along the Sangihe Islands arc, north of Sulawesi Island. Figure 1 shows the location of Mount Ruang. The Ruang Island itself is a small island of 4 x 5 km^2 area, to the southwest of the larger Tagulandang Island across a small strait[20]. Numerous explosive eruptions of Ruang have been documented since 1808. Ruang is a stratovolcano with a height of 725 meters. The dome-shaped feature on top of Ruang is the result of highly viscous lava that has been extruded and cooled in the vicinity of the vent[21]. The pressure within the viscous magma inside lava domes is typically linked to explosive eruptions[22].

This volcano had been dormant for around 22 years with its previous eruption occurring in 2002, which caused damage to settlements and agricultural land, resulting in 1000 people evacuated to nearby islands[2]. Meanwhile, historically, the most catastrophic eruption of Ruang volcano happened in 1871, which caused a tsunami that resulted in the deaths of over 400 people[1]. On 16 April 2024, Ruang volcano, which is located on Ruang Island, Tagulandang District, North Sulawesi, Indonesia, erupted just a few hours after the government raised the status to alert level. The eruption was a great explosive event that expelled lava, ash, sulfur dioxide, and other volcanic materials. A few days later, the alert status of Ruang volcano was downgraded to a beware level. However, on 30 April 2024, another significant explosion occurred. During the second eruption, a shower of volcanic rocks impacted massive areas surrounding the island, leading to the closure of Sam Ratulangi Airport, located approximately 97.3 kilometers away. The eruption also expelled SO2 which reached other islands, as far as Kalimantan. There are roughly 878 people living within a 5-kilometer radius, and 1,652 people living within a 10-kilometer radius.

2.2. Data

2.2.1. SPOT 7

SPOT (Satellite pour l'Observation de la Terre) is a commercial remote sensing satellite[23]. The latest satellite of SPOT series is SPOT 7 which was launched on 1 June 2014 and stopped its operation on 17 March 2023. SPOT 7, together with SPOT 6, are the latest identical satellite systems in the SPOT satellite series which guarantee continuous data with high resolution and wide swath. SPOT 7 imagery consists of two modes, namely the panchromatic mode which consists of 1 band with 1.5 meters spatial resolution, and the multispectral mode

Cite: D. Monica et al., "Rapid Mapping of Morphological Change Following the 2024 Ruang Volcano Eruption Using Multi-sensor Remote Sensing Imagery". Evergreen, 12 (03) 1426-1437 (2025). https://doi.org/10.5109/7388839.

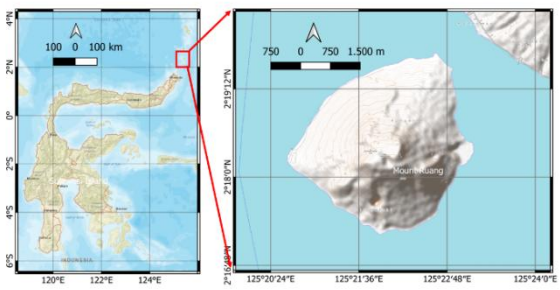

Fig. 1: Mount Ruang located on a small island above Sulawesi, as seen from Sentinel-2 data acquired on February 17th 2024

which consists of 4 bands in the visible and near-infrared electromagnetic spectrum with 6 meters spatial resolution. The SPOT imagery used in this study is the relatively cloud-free SPOT 7 images acquired on 12 June 2019 and 10 January 2022. This data is used to see whether there were significant changes in the shoreline around Ruang Island within those two years.

2.2.2. PlanetScope

PlanetScope (PS) is a constellation of satellites owned by Planet Labs (PL). As of early 2019, PlanetScope consists of more than 150 CubeSats called 'Doves', each approximately sized 10 × 10 × 30 cm (also called three units or 3U CubeSats)[24]. This constellation orbits in two near poles, sun-synchronous orbits with ~8◦ and ~98◦ inclination at an altitude of ~475 km. PlanetScope imagery has a resolution of 3m and different multispectral bands, namely Red, Green, Blue, and Near InfraRed. PlanetScope acquires data every day through its doves so that cloudy data on one day can be immediately replaced by data recorded the next day[25,26]. These features, together with an open data access policy for research purposes, make PlanetScope data attractive for surface change monitoring of dynamic geophysical events such as volcanic activity. More detailed specifications of PlanetScope imagery are presented in Table 1.

Table 1: Specifications of PlanetScope imagery.

Sensor Type	Four-band frame Imager with a split-frame VIS+NIR filter
Spectral Bands: Blue Green Red NIR	 455 - 515 nm 500 - 590 nm 590 - 670 nm 780 - 860 nm
Ground Sample Distance (nadir)	3.0 m-4.1 m (approximate, altitude dependent)
Frame Size	24 km x 8 km (approximate)
Maximum Image	20,000 km²
Strip per orbit	
Revisit Time	Daily at nadir
Image Capture Capacity	200 million km²/day

2.2.3. Sentinel-1A

For this study, we utilized three scenes from the Sentinel-1A dataset. Sentinel-1A is a satellite operated by the European Space Agency (ESA), which was launched in 2014[27]. Sentinel-1A satellites provide Synthetic Aperture Radar (SAR) data, which is ideal for constant monitoring in all types of weather regardless of cloud and haze[28]. The revisit time for Sentinel-1A is 12 days.

Table 2: Specifications of Sentinel-1A data used in this study.

Acquisition date	Mode	Direction	Path
14 April 2024	SLC	Descending	163
14 April 2024	GRD	Descending	163
26 April 2024	SLC	Descending	163
26 April 2024	GRD	Descending	163
8 May 2024	SLC	Descending	163
8 May 2024	GRD	Descending	163

Table 3: Interferometric pairs used in this study.

Acquisition dates	Baseline (m)
14 April - 26 April	354
26 April - 8 May	82
14 April - 8 May	436

The data used in this study are Single Look Complex (SLC) and Ground Range Detected (GRD) with Interferometric Wide (IW) swath mode. This mode has a 250 km swath width and moderate resolution of 5 m by 20 m[27]. The acquisition dates for the data are 14 April, 26 April, and 8 May 2024; which are the closest dates Sentinel-1A dataset can provide regarding the 2024 Ruang eruption. Detailed specifications for each scene and pair that will be used in the interferometric analysis are presented in Table 2 and Table 3.

2.3. Methods

The overall methods are outlined in Figure 2. The following subheadings describe the approach used to detect the morphological changes, which included shoreline and terrain changes.

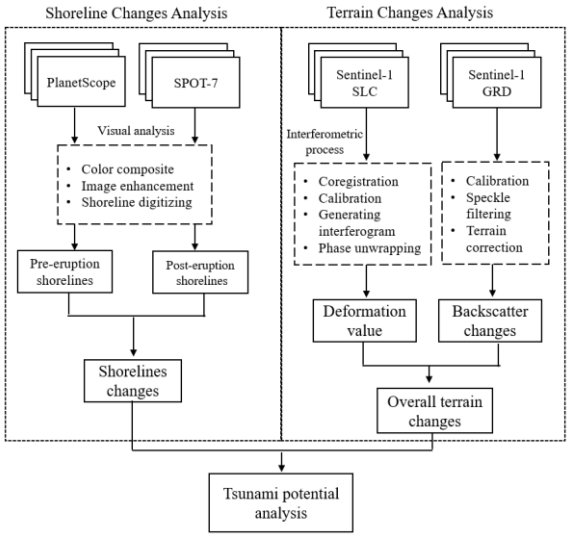

Fig. 2: Flowchart methods

2.3.1. Shoreline changes analysis using SPOT and Planet data

This analysis was carried out visually (visual delineation) of the shorelines before and after the eruption. PlanetScope data is available before the eruption. SPOT-7 data is available after the eruption. Before visual delineation, both images are processed through color composite and image enhancement.

The Planet Explorer interface was utilized to browse PlanetScope images and download items. We located, examined for cloud cover and clarity, and downloaded images taken before and after the 1st and 2nd eruption on 24 April and 4 May 2024. Using appropriate RGB color stretching values[29] to draw attention to volcanic deposits and structures, visual assessment of the photos was accomplished. Visual comparison of pre, 1st and 2nd eruption were performed to identify the shoreline change, including new deposits produced by the Ruang eruption. The visible bands were mostly employed for visual comparisons, but in certain cases the NIR band was also used (in substitution for the blue band in the RGB composite photos), especially where there were changes in the vegetation cover as a result of the volcanic activity. All datasets in this part were processed using Quantum GIS software.

2.3.2. Terrain changes analysis using Sentinel-1A data

The terrain changes analysis is conducted with two approaches, one is interferogram analysis using Sentinel-1A SLC data[30] and the other is backscatter change detection using Sentinel-1A GRD data[31].

Interferometric analysis is used to detect ground deformation between two different acquisitions of two SAR images. With regard to volcano monitoring, this method is useful to measure volcano inflation and deflation, as well as eruption-induced subsidence and landslides [32].

The backscatter approach analyzes the strength of radar echo in various surfaces, which is ideal for detecting the existence of eruption materials covering the ground, such as ash, lava, and deposits[33]. For this research we use sigma naught value, which is the radar reflectivity per unit area in ground range[34]. Sigma naught (σ^0) value is affected by how the ground surface is angled relative to the sensor and how far it is from the sensor. Thus, the calculation of sigma naught requires an information on the local slope or incidence angle, as shown in Equation 1[34].

$$\sigma^0 = (k_S.|DN|^2 - NEBN).\sin\theta_{loc} \qquad (1)$$

Where k_S is the scaling factor, DN is pixel intensity value, NEBN is Noise Equivalent Beta Naught or influence of different noise contribution to the signal, and θ_{loc} is the local incidence angle.

Before conducting the interferogram analysis, we apply preprocessing steps first. The first step in preprocessing Sentinel-1A SLC data is to apply orbit files. The orbit files provide information about the satellite's precise position and velocity at the time of data acquisition. This step improves the accuracy of the initial geolocation data. After applying the orbit files, the next step is to coregister pairs of two Sentinel-1A images in order to align them so that each pixel corresponds to the same ground location. For this study, we registered three pairs of data i.e 14 April-26 April, 26 April-8 May, and 14 April-8 May. After, a calibration process is conducted which includes several steps to enhance the quality of the data. First calibration step is Enhanced Spectral Diversity (ESD) to improve accuracy using spectral differences between multiple bursts within the Sentinel-1A image. Next is the removal of the topographic phase using a Digital Elevation Model (DEM), leaving only the phase information related to ground movement. Next, Goldstein filter and adaptive filters are used in this process to improve the signal-to-noise ratio of the interferogram. Interferogram of a radar data is generated by calculating the phase difference between the master image and slave image. Unwrapping is a process to convert the phase difference into a continuous surface value, which represents the total displacement[35]. After the unwrapping process, the phase value is converted to displacement value. The entire process is done on ESA SNAP Program.

Meanwhile, the pre-processing steps for backscatter analysis include applying orbit file, calibration, speckle filtering, and terrain correction. Orbit file is applied to Sentinel-1A GRD data in order to increase the accuracy of the satellite's position and velocity at the time of data acquisition. Next, the data is calibrated to obtain the backscatter values. Goldstein filter is used to reduce the noise in the data, and finally terrain correction is applied to fix the geolocation error. The change detection analysis is conducted by creating a false-color RGB image using the

backscatter values, where the later date is assigned on the red channel, and the earlier date is assigned on the green channel. We create three pairs of images namely 14 April-26 April, 26 April-8 May, and 14 April-8 May pairs.

2.3.3. Tsunami potential analysis

Tsunami potential analysis is carried out based on the results of terrain analysis. Given that the Ruang Volcano is a volcanic island surrounded by coastal and sea waters, the occurrence of terrain changes has implications for the tsunami potential.

Understanding the morphological changes induced by volcanic activity, especially in island arc settings, is critical for assessing potential tsunami generation mechanisms[36]. This analysis provides a means to identify hotspots of significant morphological change, which can then be further investigated for their potential to generate tsunamis[37]. Such detailed monitoring of terrain and shoreline changes, especially with high-resolution satellite imagery, is fundamental for developing accurate landslide inventories and assessing seismic landslide hazards[38]. This is particularly relevant for understanding the potential for volcano-induced landslides and flank collapses, which are significant contributors to tsunami generation[38].

3. Results and Discussions

Our analysis demonstrates that the integration of PlanetScope optical imagery with Sentinel-1A synthetic aperture radar (SAR) data provides a strong complementary dataset sufficient for near real-time monitoring of Mount Ruang during the 2024 eruptive event. The following subsections explain the individual capabilities and contributions of the PlanetScope and Sentinel-1A datasets in capturing and analyzing changes that took place during the 2024 eruption.

3.1. Assessment on remote sensing data availability

Since volcanic activity is still mostly unpredictable and might result in dynamic phenomena that can be challenging to watch and analyze in real-time during quickly changing crisis scenarios, temporal resolution is perhaps the most important factor. The ability to conduct rapid mapping of disasters such as the Ruang eruption relies on the availability of multi remote sensing data from different temporal resolutions. There is often a trade-off between temporal and spatial resolution, such as data with high temporal resolution having lower spatial resolution, and vice versa. Therefore, an integration of multisensor is necessary to ensure near real-time monitoring and analysis of volcanic disasters. In this case, the availability of several remote sensing datasets in capturing the event of 2024 Ruang eruption is shown in Figure 3.

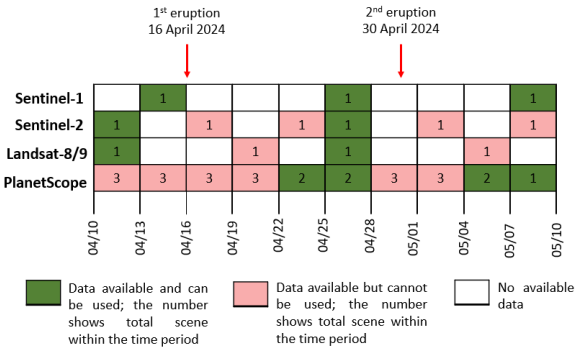

Fig. 3: Remote sensing data availability for 2024 Ruang Volcano eruption from 10 April to 10 May 2024

Sentinel-1A provides data every 12 days. Unfortunately, the first Ruang eruption occurred just two days after the Sentinel-1A satellite last passed over the area. As a result, we had to wait for 10 days to obtain post-eruption data from Sentinel-1A. Luckily, this data is guaranteed to be usable, as Sentinel-1A offers a significant advantage, that is, its ability to penetrate cloud cover, ash plumes, and smoke. Radar imagery is also sensitive to surface roughness, moisture content, and structural changes, enabling the detection of morphological changes and deformation even under bad weather conditions or during nighttime.

On the other hand, PlanetScope offers daily high-resolution data with a ground sampling distance of approximately 3–4.1 meters, as opposed to Sentinel-1A which has a coarser spatial resolution of 5 x 20 meters. PlanetScope's high resolution allows for the detection of fine-scale features and subtle shoreline modifications. It is also the better option compared to other optical remote sensing data such as Landsat or Sentinel-2, as PlanetScope excels in higher temporal resolution and higher spatial resolution. However, not all the daily acquired data can be utilized effectively as many of them are covered in cloud and haze. This is where Sentinel-1A data comes in handy. When used together, the high spatial detail of PlanetScope and the all-weather, day-and-night imaging capabilities of Sentinel-1A complement each other effectively. The optical data provide fine-grained spatial context and visual clarity of shoreline features, while radar data enhance temporal continuity and enable the observation of physical changes in topography and surface structure.

3.2. Shoreline changes detection

Daily time series PlanetScope data of the first eruption, visualized as composite image of 4-3-2 band combination, was able to detect the presence of material deposits in the form of pyroclastic flows deposited on the north, northeast and east (N, NE, E) slopes of the Ruang volcano's flanks, as seen in Figure 4. On the eastern slope (E), pyroclastic material was identified to be moving from the peak down the slope following the main channel until it reached the shoreline.

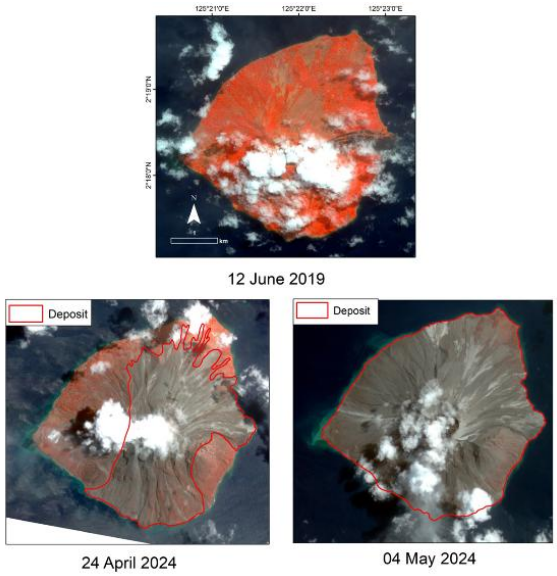

Fig. 4: Time series multisensor remote sensing imagery of Ruang Volcano, from left to right: before eruption, post first eruption, post second eruption

Daily time series PlanetScope data of the first eruption, visualized as a composite image of 4-3-2 band combination, was able to detect the presence of material deposits in the form of pyroclastic flows deposited on the north, northeast, and east (N, NE, E) slopes of the Ruang volcano's flanks, as seen in Figure 4 (24 April 2024). On the eastern slope (E), pyroclastic material was identified to be moving from the peak down the slope following the main channel until it reached the shoreline.

Material in the form of a mix of tephra fall and pyroclastic flow was also identified to be falling and covering the vegetation land cover on the southern (S) slope. On the southern slope, vegetation covered by falling volcanic material remains discernible due to the image's subtle red color from April 24, 2024. There is less material deposited on this slope than on the N flank area, as evidenced by the vegetation that is still recognizable.

The first eruption showed the dominant material moving to the north and northeast and slightly to the south. Vegetation and settlements can be identified on the western slopes, slightly covered by thin volcanic ash falls. Image after the second eruption, acquired on 4 May 2024, shows a more even distribution of volcanic materials on the Ruang Island. Distinction of pyroclastic material, lava flows and ash or tephra falls can no longer be clearly identified on PS images after this eruption. Material deposits have reached all sides of the Ruang volcano to all sides of the shoreline of the Ruang island.

Shoreline changes in both eruption events can be identified through PlanetScope's daily imagery data. The changes that occurred on the east side of Ruang Island were well detected, especially the changes after the first eruption (17 April 2024). The shoreline changes are marked by the volcanic material reaching the red line (post-eruption

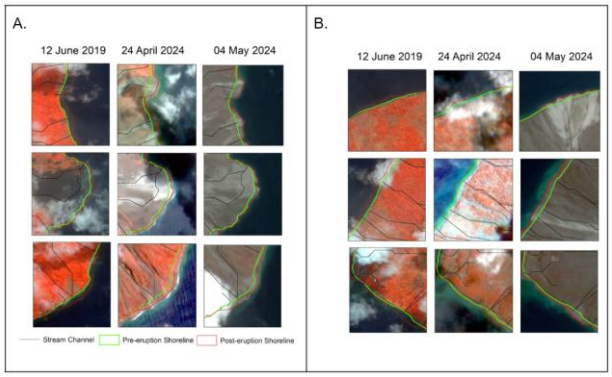

Fig. 5: Shoreline changes a) East coast of Ruang Volcano and b) West coast of Ruang Volcano:, from left to right: before eruption, post first eruption, post second eruption

Subsequently, after the second eruption, both the north and east coasts of Ruang Island did not show any changes. Most of the eruptive materials from the second eruption presumably went to the west side of the island. Furthermore, the west shoreline of Ruang Island was detected to have only changed after the second eruption on 30 April 2024. Changes mostly occurred at the end of channels that originate near the crater of Ruang Volcano. The maximum addition of shoreline on the east and west coasts varies, reaching 20-70 m from the original shoreline. In the east, the detected shoreline changes are on average greater than on the west side.

shoreline). The three channels that went downstream to the east coast of Ruang Island, as shown in Figure 5, indicates that there are terrain changes caused by eruption material during the first eruption.

Figure 6 shows that there are hills shaped like the remains of andesitic lava flow. These hills are remnants of old lava flow activity that were exposed after the vegetation covering them collapsed after being crushed by eruptive material moved southward. Although this morphology is not visible in pre-event imagery, the geological map (PVMBG, 2008) shows that this feature has existed since before the 2024 eruption. The loss of vegetation on the southern slopes exposes the morphology of this ridge.

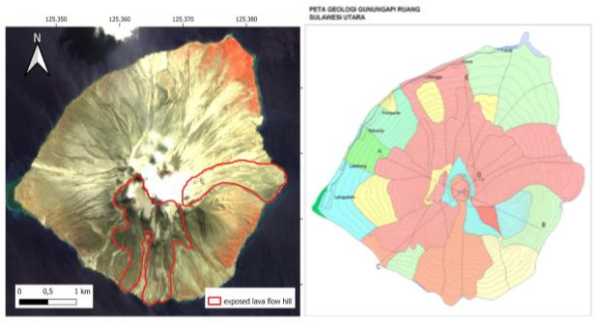

Fig. 6: PlanetScope image acquired on 19 May 2024 (left) and Ruang volcano geological map (right)

Cite: D. Monica et al., "Rapid Mapping of Morphological Change Following the 2024 Ruang Volcano Eruption Using Multi-sensor Remote Sensing Imagery". Evergreen, 12 (03) 1426-1437 (2025). https://doi.org/10.5109/7388839.

3.3. Terrain changes

Figure 7 shows the backscatter value changes between three pairs of data which represent the condition before and after the first and second eruption of Ruang volcano.

Backscatter value, usually expressed in decibels (dB), represents the strength of the radar signal which reflected back to the satellite. As such, this value is sensitive to surface's texture. The increase in surface roughness, moisture, or structural heterogeneity will also increase the backscatter value. Likewise, the decrease in surface fineness or vegetation cover will decrease the backscatter value as well.

In Figure 7(a), the first eruption raised the backscatter values on the northern and southern sides of the volcano crater, which suggests the existence of coarse pyroclastics materials expelled from the crater and scattered throughout the north and south directions. Twelve days later, however, after the second eruption, the backscatter values decreased as seen in Figure 7(b). This suggests that finer ashes and tephra that previously scattered in the air have finally settled on the land. Figure 7(c) shows overall surface changes through the first and second eruptions, indicating the areas impacted by the expelled volcanic materials. The backscatter values of the western side of the island remains unchanged, which indicates that most of the pyroclastic materials were expelled to the other sides.

Figure 8 shows the deformation between three pairs of Sentinel-1A data which represent the condition before and after the first and second eruption of Ruang volcano. The deformation between 14 April and 26 April shows how the first eruption changed the terrain (Figure 8(a)). An elevation decrease happened around the crater, which indicates that volcanic material under the surface was expelled from the crater during the eruption, causing the ground surface around the crater to decrease. The lowest terrain decrease during this timeframe was -0.434 meters. Meanwhile, the 0.072 meters increase on the northern shoreline can be attributed to the volcanic material deposits such as ash and incandescent rocks flowing from the crater to the north direction. The changes that occurred after the second eruption are depicted by the deformation between 26 April and 8 May (Figure 8(b)). The larger area of elevation decreased around the crater extending from north to south indicates a greater impact of the eruption. The increase in elevation also extended to the eastern area compared to the previous eruption. This result indicates additional volcanic material deposits as well as changes in the pyroclastic flow direction.

Ruang Volcano, an active stratovolcano in North Sulawesi, lies within a tectonically complex area where the Eurasian, Pacific, and Philippine plates meet, resulting in intense seismic and volcanic activity.

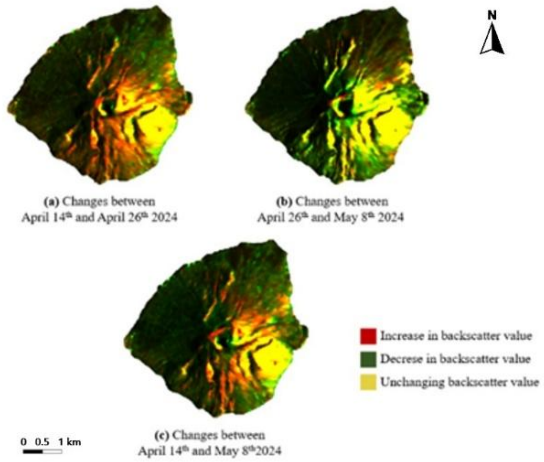

Fig. 7: Backscatter value changes between pre-eruption date and post-eruption dates

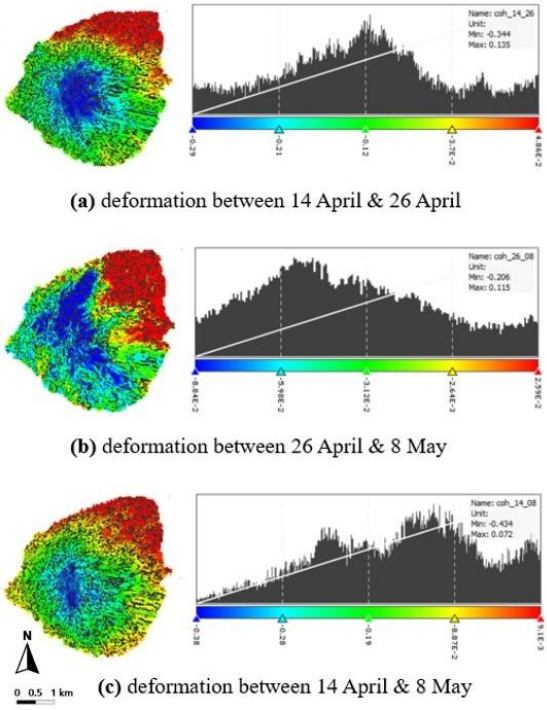

Fig. 8: Deformation of the surface of Ruang volcano surrounding between pre-eruption date and post-eruption dates

Changes in the volcano's terrain surface serve as key indicators of underground magma behavior, reflecting magma accumulation, movement, and pressure changes. Prior to its April 2024 eruption, Ruang experienced a noticeable rise in deep volcanic earthquakes and gravel emissions, suggesting magma migration, rock fracturing, and a notable cooling of the volcano's interior.

For analysis purpose, we divided the Ruang island into five sections, namely the crater, the northern side, the eastern side, the southern side, and the western side. We calculates the statistics of morphological changes in each section. The overall changes in the backscatter values, deformation, and shorelines is shown in Table 4.

Cite: D. Monica et al., "Rapid Mapping of Morphological Change Following the 2024 Ruang Volcano Eruption Using Multi-sensor Remote Sensing Imagery". Evergreen, 12 (03) 1426-1437 (2025). https://doi.org/10.5109/7388839.

Table 4: Summary of changes in Mount Ruang and its surrounding by the 2024 Eruption

Parameter		Eruption 1st					Eruption 2nd				
		Crater	Slope				Crater	Slope			
			Northern	Eastern	Southern	Western		Nortern	Eastern	Southern	Western
Backscatter (dB)	Min	-15.508	-16.923	-9.849	-5.666	-12.814	-18.836	-21.132	-16.344	-16.678	-14.996
	Max	20.998	21.177	21.205	17.29	11.029	17.91	13.197	16.06	14.58	13.307
	Avg	2.375	-0.203	2.176	2.633	-0.628	-2.896	-1.185	0.262	-1.631	-2.771
Deformation (m)	Min	-0.326	-0.341	-0.248	-0.328	-0.35	-0.128	-0.206	-0.076	-0.124	-0.157
	Max	-0.143	0.138	0.094	0	0	0.017	0.112	0.115	0.027	0.022
	Avg	-0.25	-0.041	-0.081	-0.147	-0.178	-0.057	-0.008	0.006	-0.055	-0.058
Net Shoreline Movement (m)	Min							8.019	12.11	0.127	8.664
	Max							40.631	82.76	3.459	53.411
	Avg							25.88138	47.5566	1.109947	36.13045

3.4. Integration of multi-sensor remote sensing abilities for volcano monitoring

The combination of Sentinel-1A's radar data and both SPOT-7's and PlanetScope's visible data serves as complementary tools for volcanic events monitoring. In this case of Ruang volcano, Sentinel-1A provides constant monitoring of Ruang volcano and is able to capture situations during the eruption despite the existence of massive ash plumes, as well as detect terrain changes caused by the eruption. Meanwhile, PlanetScope data provided detailed visual information which is necessary for detecting pyroclastic flow and ash deposits, as well as analyzing shoreline changes and vegetation changes.

From the PlanetScope data, it can be seen that the first eruption of Ruang volcano has caused 20-70 meters changes in the east shorelines. This finding is also supported by the SAR deformation analysis, which shows elevation rise in the eastern side of Ruang island and changes in the entire island. Later in the second eruption, both the PlanetScope and Sentinel-1A backscatter data show that materials fell to a wider area on the west and north, making almost the entire island covered in ash and other pyroclastic materials. To sum up, PlanetScope data captures the horizontal aspects of Ruang's morphological changes, including the shoreline changes due to volcanic deposits and the direction of ash plumes and other eruptive materials. Meanwhile Sentinel-1A data measures the vertical aspects such as the uplift and subsidence on Ruang island before and after the eruption, which are related to the magma movement under the surface. The backscatter analysis shows the coverage of the pyroclastic materials toward the island's surface. The onsite monitoring after the second eruption (Figure 9) supports this finding as it can be seen that the fresh pyroclastic materials (greyscale color) covered the entire northern part of the island.

This study shows that by combining these two different datasets, we can obtain a comprehensive understanding of Ruang volcanic incident in a timely manner. The first eruption happened on 16 April, followed by the second eruption on 30 April. The earliest clear data we can obtain is PlanetScope data acquired on 24 April and Sentinel-1A data acquired on 26 April, which means that we are able to provide information within a week of the first eruption.

3.5. Early warning tsunami due to deposit material

Ground deformation and terrain changes are indicators of potential landslides, which can have disastrous impacts when occurring near shorelines or underwater. When such

Fig. 9: Photograph of the second eruption of Ruang volcano observed from north direction, provided by Magma PVMBG (https://magma.vsi.esdm.go.id/)

landslides happen, it can displace a large volume of water and potentially trigger a tsunami. This study has observed that ground deformation and terrain changes occurred on Ruang island as a result of the 2024 Ruang eruption. The 7.2 centimeters to 13.5 centimeters subsidence around the Ruang volcano crater indicates magma movement beneath the surface, which suggests unstable volcanic structure. Furthermore, volcanic deposits have been found to pile most on the north and east shores of Ruang island, to the point of extending the shorelines 20-70 meters outward. These volcanic deposits of ash and other pyroclastic materials can bring pressure onto the slopes and increase its instability. The combination of these two occurrences may increase the potential of landslides especially near the north and east shorelines. If the landslides occur it can cause materials to fall on the ocean and therefore generate tsunami. Previous research conducted by Grilli et al., in the case of the 2018 Anak Krakatau tsunami, has also shown that terrain changes in the coastal areas due to the accumulation of eruption material deposits, lava and pyroclastic, in significant quantities, are an indication of the potential for a tsunami[39].

4. Conclusions and Recommendations

This study found that integrating high-resolution PlanetScope optical imagery with Sentinel-1A SAR data is a sufficient approach to comprehensively assess volcanic hazards, particularly in remote island settings where in-situ observations are limited. By combining the strengths of both sensor types we were able to detect significant coastal changes, including shoreline expansion of up to 70 meters and vertical surface displacements ranging from −0.434 to 0.072 meters. These observed geomorphological shifts are not only indicative of the dynamic nature of Ruang Volcano's activity but also serve as potential precursors to more severe secondary hazards, such as tsunamis.

On the other hand, while remote sensing technology has proved its ability in providing us with comprehensive information necessary for volcano monitoring, there are still several drawbacks that should be addressed. For the PlanetScope data, the visual analysis is conducted manually and therefore requires relatively more time and effort. There is also limitation in its electromagnetic spectrum, where PlanetScope data contain only four bands of visual and NIR. On the other hand, Sentinel-1A data robustness is limited by our study area which is mainly covered in vegetation, as vegetation cover reduces the interferometric coherence. Moreover, the accuracy of InSAR analysis also depends on the perpendicular and temporal baselines of each data pair. As this study conducts a quick response monitoring, we use the earliest available data despite the baseline value not being the most optimal for an InSAR analysis.

To overcome the limitations above, several points can be considered in future studies. First is to implement advanced machine learning techniques to automatically detect and classify volcanic deposits using high-resolution PlanetScope data, as opposed to manual visual interpretation which requires more time and effort to conduct. This approach can help in rapidly analyzing large datasets in shorter times. A field observation is also recommended in future studies to validate the results obtained from the remote sensing analysis, in order to enhance the reliability of the remote sensing interpretations. As for the remote sensing analysis itself, time series methods such as Small Baseline Subset[40] or Persistent Scatterer Interferometry[41] can be considered for more precise anomalies detection.

Strong collaboration with PVMBG and other relevant Indonesian ground monitoring agencies is essential to conduct a thorough, precise, and meaningful analysis of the morphological changes from the 2024 Ruang Volcano eruption using multi-sensor remote sensing imagery. This partnership will enhance scientific insight and support the development of more effective disaster mitigation strategies.

Incorporating the analysis of morphological changes after the 2024 Ruang Volcano eruption—derived from multi-sensor remote sensing imagery—into national disaster management platforms such as InaTEWS and MAGMA Indonesia can greatly strengthen volcanic hazard monitoring and early warning systems. Utilizing real-time or near-real-time remote sensing data allows authorities to quickly detect surface deformation, lava flow trajectories, changes in crater structure, and coastal alterations. These insights are crucial for evaluating eruption severity and anticipating related hazards like tsunamis, landslides, and pyroclastic flows. When integrated with existing seismic, geodetic, and gas emission data, this approach contributes to a more comprehensive, data-informed decision-making framework. Furthermore, remote sensing outputs can enhance automated alert systems, hazard mapping, and information dissemination processes—ultimately leading to faster emergency responses and improved public safety during volcanic events.

Author Contributions

Conceptualization, D.M, I.M., and A.T.; Methodology, S. Suwarsono, D.M., and I.M.; Investigation, F.C. and R.D.I.; Resources, R. and S. Suhermat; Writing -- Original Draft, D.M. and I.M.; Writing - Review & Editing, S Suwarsono and Y.V.; Validation, H.D.P. and H.D.; Supervision, Y.V. and A.T.

References

1) E.U. Zorn, A. Orynbaikyzy, S. Plank, A. Babeyko, H. Darmawan, I.F. Robbany, and T.R. Walter, “Identification and ranking of volcanic tsunami hazard sources in southeast asia,” EGUsphere, 2022

1–38 (2022). doi:10.5194/egusphere-2022-130.

2) A. Hidayat, M.A. Marfai, and D.S. Hadmoko, "Eruption hazard and challenges of volcanic crisis management on a small island: a case study on ternate island - indonesia," Int. J. GEOMATE, 18 (66) 171–178 (2020). doi:10.21660/2020.66.ICGeo43.
3) H.Z. Abidin, H. Andreas, M. Gamal, M.A. Kusuma, M. Hendrasto, O.K. Suganda, M.A. Purbawinata, F. Kimata, and I. Meilano, "Volcano Deformation Monitoring in Indonesia: Status, Limitations and Prospects BT - Dynamic Planet: Monitoring and Understanding a Dynamic Planet with Geodetic and Oceanographic Tools IAG Symposium Cairns, Australia 22–26 August, 2005," in: P. Tregoning, C. Rizos (Eds.), Springer Berlin Heidelberg, Berlin, Heidelberg, 2007: pp. 790–798. doi:10.1007/978-3-540-49350-1_113.
4) G. Saccorotti, M. Iguchi, and A. Aiuppa, "Chapter 7 - In situ Volcano Monitoring: Present and Future," in: J.F. Shroder, P.B.T.-V.H. Papale Risks and Disasters (Eds.), Hazards Disasters Ser., Elsevier, Boston, 2015: pp. 169–202. doi:https://doi.org/10.1016/B978-0-12-396453-3.00007-1.
5) D. Coppola, M. Laiolo, C. Cigolini, F. Massimetti, D. Delle Donne, M. Ripepe, H. Arias, S. Barsotti, C.B. Parra, R.G. Centeno, S. Cevuard, G. Chigna, C. Chun, E. Garaebiti, D. Gonzales, J. Griswold, J. Juarez, L.E. Lara, C.M. López, O. Macedo, C. Mahinda, S. Ogburn, O. Prambada, P. Ramon, D. Ramos, A. Peltier, S. Saunders, E. de Zeeuw-van Dalfsen, N. Varley, and R. William, "Thermal remote sensing for global volcano monitoring: experiences from the mirova system," Front. Earth Sci., 7 (2020). doi:10.3389/feart.2019.00362.
6) F. Cigna, D. Tapete, and Z. Lu, "Remote sensing of volcanic processes and risk," Remote Sens., 12 (16) (2020). doi:10.3390/RS12162567.
7) G. Ganci, A. Cappello, G. Bilotta, and C. Del Negro, "How the variety of satellite remote sensing data over volcanoes can assist hazard monitoring efforts: the 2011 eruption of nabro volcano," Remote Sens. Environ., 236 (September 2019) 111426 (2020). doi:10.1016/j.rse.2019.111426.
8) D. McAlpin, and F.J. Meyer, "Multi-sensor data fusion for remote sensing of post-eruptive deformation and depositional features at redoubt volcano," J. Volcanol. Geotherm. Res., 259 414–423 (2013). doi:https://doi.org/10.1016/j.jvolgeores.2012.08.006.
9) M.A. Furtney, M.E. Pritchard, J. Biggs, S.A. Carn, S.K. Ebmeier, J.A. Jay, B.T. McCormick Kilbride, and K.A. Reath, "Synthesizing multi-sensor, multi-satellite, multi-decadal datasets for global volcano monitoring," J. Volcanol. Geotherm. Res., 365 38–56 (2018). doi:https://doi.org/10.1016/j.jvolgeores.2018.10.002.
10) C.A. Suarez-Herrera, G. Toyos, L.J. Candela-becerra, M. Agusto, and A. Su, "Journal of south american earth sciences analysis of thermal anomalies at copahue volcano between october 2011 and the december 2012 eruption with modis," 110 (April) (2021). doi:10.1016/j.jsames.2021.103310.
11) D. Coppola, D. Piscopo, M. Laiolo, C. Cigolini, D.D. Donne, and M. Ripepe, "Radiative heat power at stromboli volcano during 2000 – 2011 : twelve years of modis observations," J. Volcanol. Geotherm. Res., 215–216 48–60 (2012). doi:10.1016/j.jvolgeores.2011.12.001.
12) D. Coppola, M. Laiolo, A. Campus, and F. Massimetti, "Thermal unrest of a fumarolic fi eld tracked using viirs imaging bands : the case of la fossa crater (vulcano island , italy)," (August) 1–9 (2022). doi:10.3389/feart.2022.964372.
13) A. Campus, M. Laiolo, F. Massimetti, and D. Coppola, "The transition from modis to viirs for global volcano thermal monitoring," Remote Sens., 12 (2567) (2020). doi: https://doi.org/10.3390/s22051713
14) F. Massimetti, D. Coppola, M. Laiolo, S. Valade, C. Cigolini, and M. Ripepe, "Volcanic hot-spot detection using sentinel-2 : a comparison with modis – mirova thermal data series," (2020). doi: https://doi.org/10.3390/rs12050820.
15) C. Corradino, E. Amato, F. Torrisi, and C. Del Negro, "Data-driven random forest models for detecting volcanic hot spots in sentinel-2 msi images," Remote Sens., 14 (17) 1–18 (2022). doi:10.3390/rs14174370.
16) N. Zaini, M. Yanis, F. Abdullah, F. Van Der Meer, and M. Aufaristama, "Exploring the geothermal potential of peut sagoe volcano using landsat 8 oli/tirs images," Geothermics, 105 (November 2021) 102499 (2022). doi:10.1016/j.geothermics.2022.102499.
17) J.Biggs, F. Dogru, A. Dagliyar, F. Albino, S. Yip, and S. Brown, "Baseline monitoring of volcanic regions with little recent activity : application of sentinel-1 insar to turkish volcanoes," J Appl. Volcanol., 1–14 (2021). doi: https://doi.org/10.1186/s13617-021-00102-x
18) R. Tiengo, J.M.R. Pacheco, and A. Gil, "Using sentinel-1 grd sar data for volcanic eruptions monitoring : the case- study of fogo volcano (cabo verde) in 2014 / 2015," (December) (2021).
19) A. Valjarević, C. Morar, J. Živković, L. Niemets, D. Kićović, J. Golijanin, M. Gocić, N.M. Bursać, L. Stričević, I. Žiberna, N. Bačević, I. Milevski, U. Durlević, and T. Lukić, "Long term monitoring and connection between topography and cloud cover distribution in serbia," Atmosphere (Basel)., 12 (8)

(2021). doi:10.3390/atmos12080964.

20) M.M.F. Rampengan, A.K. Boedhihartono, L. Law, J.C. Gaillard, and J. Sayer, "Capacities in facing natural hazards: a small island perspective," Int. J. Disaster Risk Sci., 5 (4) 247–264 (2014). doi:10.1007/s13753-014-0031-4.
21) Y.V Starodubtseva, I.S. Starodubtsev, A.T. Ismail-Zadeh, I.A. Tsepelev, O.E. Melnik, and A.I. Korotkii, "A method for magma viscosity assessment by lava dome morphology," J. Volcanol. Seismol., 15 (3) 159–168 (2021). doi:10.1134/S0742046321030064.
22) L. Caricchi, M. Townsend, and E. Rivalta, "The build-up and triggers of volcanic eruptions," Nat. Rev. Earth Environ., 2 (July) (2021). doi:10.1038/s43017-021-00174-8.
23) M. Chevrel, M. Courtois, and G. Weill, "The spot satellite remote sensing mission," Photogramm. Eng. Remote Sensing, 47 1163–1171 (1981).
24) A.E. Frazier, and B.L. Hemingway, "A technical review of planet smallsat data : practical considerations for processing and using planetscope imagery," (2021). doi:https://doi.org/10.3390/rs13193930
25) D.P. Roy, H. Huang, R. Houborg, and V.S. Martins, "A global analysis of the temporal availability of planetscope high spatial resolution multi-spectral imagery," Remote Sens. Environ., 264 112586 (2021). doi:https://doi.org/10.1016/j.rse.2021.112586.
26) S. Francini, R.E. Mcroberts, F. Giannetti, M. Marchetti, G.S. Mugnozza, S. Francini, R.E. Mcroberts, and F. Giannetti, "Near-real time forest change detection using planetscope imagery," Eur. J. Remote Sens., 53 (1) 233–244 (2020). doi:10.1080/22797254.2020.1806734.
27) D. Geudtner, R. Torres, P. Snoeij, M. Davidson, and B. Rommen, "Sentinel-1 System capabilities and applications," in: 2014 IEEE Geosci. Remote Sens. Symp., 2014: pp. 1457–1460. doi:10.1109/IGARSS.2014.6946711.
28) Z. Li, T. Wright, A. Hooper, P. Crippa, P. Gonzalez, R. Walters, J. Elliott, S. Ebmeier, E. Hatton, and B. Parsons, "TOWARDS insar everywhere, all the time, with sentinel-1," Int. Arch. Photogramm. Remote Sens. Spat. Inf. Sci., XLI-B4 763–766 (2016). doi:10.5194/isprs-archives-XLI-B4-763-2016.
29) J.A. Richards, and J.A. Richards, "Remote sensing digital image analysis," Springer, 2022.
30) J.C.V.-N.F.J.H.-L. Alejandro Téllez-Quiñones Adán Salazar-Garibay, and J.L. Silván-Cárdenas, "DInSAR method applied to dual-pair interferograms with sentinel-1 data: a study case on inconsistent unwrapping outputs," Int. J. Remote Sens., 41 (12) 4664–4683 (2020). doi:10.1080/01431161.2020.1727056.
31) A. Mullissa, A. Vollrath, C. Odongo-Braun, B. Slagter, J. Balling, Y. Gou, N. Gorelick, and J. Reiche, "Sentinel-1 sar backscatter analysis ready data preparation in google earth engine," Remote Sens., 13 (10) (2021). doi:10.3390/rs13101954.
32) N. Richter, and J. Froger, "The role of interferometric synthetic aperture radar in detecting , mapping , monitoring , and modelling the volcanic activity of piton de la fournaise , la r é union : a review," Remote Sens., (2020). doi: https://doi.org/10.3390/rs12061019
33) "Analyzing explosive volcanic deposits from satellite- based radar backscatter , volcán de fuego , 2018 journal of geophysical research : solid earth," Journal of Geophysical Research: Solid Earth, 126 (2018). doi:10.1029/2021JB022250.
34) AIRBUS Defence & Space, "Radiometric Calibration of TerraSAR-X Data: Beta Naught and Sigma Naught Coefficient Calculation," 2014.
35) A. Téllez-Quiñones, J.C. Valdiviezo-Navarro, and A.A. López-Caloca, "Fourier Transform Based Methods for Unwrapping of Sentinel-1 Interferograms BT - Advances in Geospatial Data Science," in: R. Tapia-McClung, O. Sánchez-Siordia, K. González-Zuccolotto, H. Carlos-Martínez (Eds.), Springer International Publishing, Cham, 2022: pp. 69–80.
36) F. Di Traglia, S. Calvari, L.D. Auria, T. Nolesini, A. Bonaccorso, A. Fornaciai, A. Esposito, A. Cristaldi, M. Favalli, and N. Casagli, "The 2014 effusive eruption at stromboli : new insights from in situ and remote-sensing measurements," Remote Sens., 10(12) (2018). doi:10.3390/rs10122035.
37) Y. Mao, D.L. Harris, Z. Xie, and S. Phinn, "Efficient measurement of large-scale decadal shoreline change with increased accuracy in tide-dominated coastal environments with google earth engine," ISPRS J. Photogramm. Remote Sens., 181 385–399 (2021). doi:https://doi.org/10.1016/j.isprsjprs.2021.09.021.
38) E.L. Harp, D.K. Keefer, H.P. Sato, and H. Yagi, "Landslide inventories: the essential part of seismic landslide hazard analyses," Eng. Geol., 122 (1) 9–21 (2011). doi:https://doi.org/10.1016/j.enggeo.2010.06.013.
39) S.T. Grilli, D.R. Tappin, S. Carey, S.F.L. Watt, S.N. Ward, A.R. Grilli, S.L. Engwell, C. Zhang, J.T. Kirby, L. Schambach, and M. Muin, "Modelling of the tsunami from the december 22, 2018 lateral collapse of anak krakatau volcano in the sunda straits, indonesia," Sci. Rep., 9 (1) 11946 (2019). doi:10.1038/s41598-019-48327-6.
40) R. Lanari, P. Berardino, M. Bonano, F. Casu, C. De Luca, S. Elefante, A. Fusco, M. Manunta, M. Manzo, and C. Ojha, "Sentinel-1 results: SBAS-DInSAR processing chain developments and land subsidence

analysis," in: 2015 IEEE Int. Geosci. Remote Sens. Symp., IEEE, 2015: pp. 2836–2839. doi: https://doi.org/10.1109/IGARSS.2015.7326405

41) M. Crosetto, O. Monserrat, M. Cuevas-González, N. Devanthéry, and B. Crippa, "Persistent scatterer interferometry: a review," ISPRS J. Photogramm. Remote Sens., 115 78–89 (2016). doi: https://doi.org/10.1016/j.isprsjprs.2015.10.011.